Chemistry–A European Journal

Supporting Information

PAINT-ing Fluorenylmethoxycarbonyl (Fmoc)-Diphenylalanine Hydrogels

Edgar Fuentes[+],[a] Kamila Boháčová[+],[a, b] Ana M. Fuentes-Caparrós,[b] Ralf Schweins,[c] Emily R. Draper,[b] Dave J. Adams,*[b] Silvia Pujals,*[a, d] and Lorenzo Albertazzi*[a, e]

SUPPORTING INFORMATION

1. Materials

FmocFF was prepared as described previously.

DMSO, d_6-DMSO and D_2O were purchased from Sigma-Aldrich. For the microscopy, gels were directly prepared in Labtek 8-well and Ibidi µ-Slide 8-well (Cat. No. 80826, Ibidi GmbH, Germany). Gels for small angle scattering were prepared in Hellma cuvettes.

2. Experimental Details

Preparation of Gels. Milli-Q water was transferred into the well and a FmocFF solution in DMSO was injected into the water drop (total 60 µL) and homogenized. Gelation took place immediately and a change of state could be observed; the solution went initially turbid, then quickly became transparent. The prepared gel was left in a humidity case overnight to ensure consistency. One hour before imaging, 150 µL of a solution with the probe at a concentration of 20-50 nM was added, maintaining the DMSO:H_2O ratio.

This procedure allowed a gel to be created with variable thickness for better imaging, but with sufficient consistency to remain assembled and attached to the glass after addition of the probe solution.

pH measurements. pH measurements of gels were assessed using a calibrated FC2020 pH probe (Hanna Instruments). The accuracy of the pH measurements is stated as ± 0.1

Confocal Microscopy. The microstructure of the gel was visualised by using a Zeiss LSM 710 confocal microscope. The sample was prepared in a CELLviewTM 35 mm plastic cell culture dish with a borosilicate glass bottom purchased from Greiner Bio-One. Nile blue A was used as fluorochrome in a concentration of 2 $\mu L \cdot mL^{-1}$ of a 0.1 w% stock solution and excited at 634 nm using a He-Ne laser (Zeiss). The objective used was a LD EC Epiplan NEUFLUAR 50x (0,55 DIC). The gel was prepared by dissolving the required amount of FmocFF (1.5 mg/mL) in DMSO in a vial, then the solution was transferred into the culture dish. Next water was added as the antisolvent to trigger gelation. The ratios of DMSO:H_2O used were 20:80 and 40:60 and the gel was prepared at a total volume of 400 µL. The gel was kept in a humid environment to prevent evaporation issues by wrapping humid tissue inside the culture dish without touching the gel and sealing it using parafilm and left overnight to gel.

Small angle neutron scattering. The gels were prepared as described above in UV spectrophotometer grade, quartz cuvettes (Hellma) with a 2 mm path length. The cuvettes were placed in a temperature-controlled sample rack during the measurements. SANS measurements were performed using the D11 instrument (Institut Laue Langevin, Grenoble, France). A neutron beam, with a fixed wavelength of 6 Å and divergence of $\Delta\lambda/\lambda$ = 9%, was used, allowing measurements over a large range in Q [$Q = 4\pi\sin(\theta/2)/\lambda$] range of 0.001 to 0.3 $Å^{-1}$, by using three sample-detector distances of 1.5 m, 8m, and 39 m.

The data were reduced to 1D scattering curves of intensity vs. Q using the facility provided software. The electronic background was subtracted, the full detector images for all data were normalized and scattering from the empty cell was subtracted. The scattering from the solvent mixture prepared using D_2O and d_6-DMSO was also measured and subtracted from the data. Most of the data were radially averaged to produce the 1D curves for each detector position. The instrument-independent data were then fitted to models using the SasView software package version.[1]

Rheology. Rheological measurements were undertaken on an Anton Paar MCR 301 rheometer. A cup and vane geometry, with a measuring gap of 1.8 mm, was used throughout to perform strain and frequency sweeps. In all cases, 2 mL gels were prepared in 7 mL Sterilin vials and left to stand overnight at room temperature before measurements. Frequency sweeps were collected at a range of frequencies varying between 1 rad s^{-1} to 100 rad s^{-1}, at a

constant strain of 0.5 %. Strain sweeps were performed from 0.1 % to 1000 % at a frequency of 10 rad s^{-1}. All the measurements were carried out at room temperature.

Super-resolution microscopy: Optical Setup. PAINT imaging was carried out with a Nikon N-STORM microscope configured for total internal reflection (TIR), using a Perfect Focus System. Irradiation under TIR conditions allowed to avoid illumination of out of focus structures, reducing background contributions and allowing for single event localizations. After laser excitation (647 nm), fluorescence was collected by a 100× 1.49 NA oil immersion objective; it passed through a quad-band dichroic mirror (97335 Nikon) and was collected by a Hamamatsu ORCA Flash 4.0 CMOS camera (pixel size 160 nm). A movie was produced where blinking generated by molecule emission appears like circular spots lasting a few acquisition frames. Three-dimensional measurements were carried out with the astigmatism method: a cylindrical lens was introduced in the light path, producing optical aberrations (elongation and inclination) of the detected fluorescence spots depending on the z-position of the emitter.

2D images were acquired at 30 ms 20-30k frames. 3D images were acquired at 30 ms, 6-10k frames, 20 stacks of 120 nm, total of 1.85 µm high.

The NIS elements Nikon software generates a list of localizations by Gaussian fitting the fluorescence spots of binding dyes in the acquired movie of diffraction-limited images. To avoid overcounting, bindings detected in consecutive frames are counted as single by the software. For 3D imaging, the z-coordinate of the localization is retrieved from the ellipticity and the inclination of the elongated spots.

Mesh quantification: ImageJ was used to analyse and measure the mesh size of the gel. The threshold of the images was adjusted so the background pixels corresponded to black pixels and fiber pixels corresponded to white pixels. The scale was set and the function “analyse particles” was run. This software basically clusters the black pixels surrounded by white pixels. Visual inspection was carried out to ensure the correct recognition of the mesh, and manual selection was also applied to include the non-recognized ones. The number of pixels/clusters are counted and transformed into area, sitting a threshold of 4 pixels to minimize the wrong identifications by the software.

Resolution calculation. Resolution Calculations STORM module in the Nikon NIS-software is able to automatically calculate the localization precision distribution for each image. As can be seen below (Figure S1), the maximum of the distribution is 9.25 nm, with most of the localizations below 9.25 nm and decreasing sharply from 9.25 nm to 11 nm.

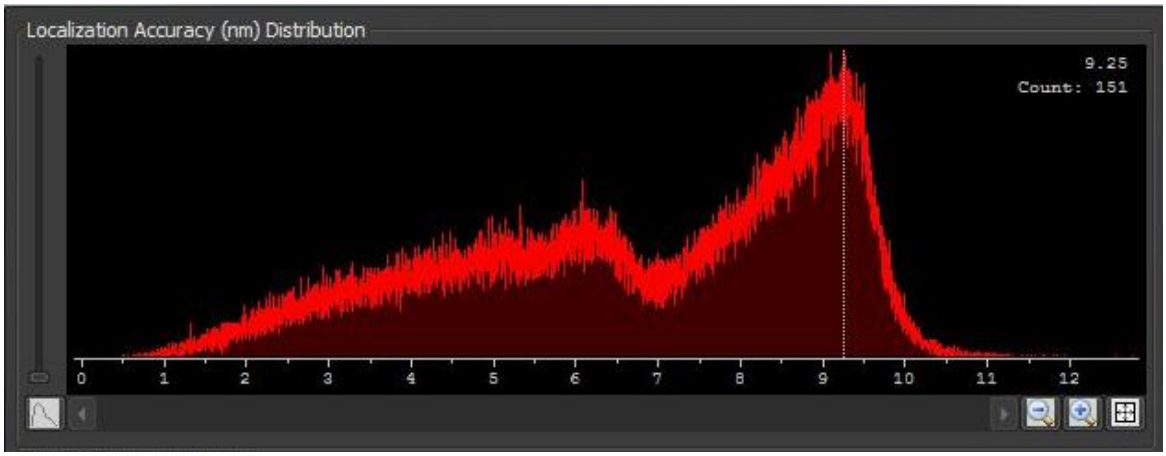

Figure S1. Localization accuracy distribution extracted from a PAINT image with the Nikon NIS-software.

These numbers are well in agreement with our calculations. The localization precision is defined as:

$$\sigma^2 = \frac{S^2 + \frac{a}{12}}{N} + \frac{8\pi^2 s^4 b^2}{a^2 N^2}$$

where,

s is the width of the PFS

N is the number of detected photons

a is the size of pixels on the camera

b is the background intensity

This can be simplified to:[2]

$$\sigma_x \geq \frac{s}{\sqrt{N}}$$

The average s for one of the images was calculated to be 246.81 ± 10.67 nm (for 218581 localizations). Also, the average for the number of photons for the same image is 606.6, with a significant population above that value. Therefore, as the average s= 246.81 nm and the average N=606.6 photons, σ_x ≥ 10.02 nm, resulting in the claimed 20 nm resolution. Single molecule localization and fitting was performed using the STORM module of NIS Elements by performing a Gaussian fitting based on the following parameters:

Minimum and maximum height: We selected the darkest bright point to be identified as a molecule and its brightness minus the background intensity was the minimum height. In our case it was set to 250. The maximum height for the used system with a sCMOS camera is 65000 and the baseline was set to 100. For the PSF, the initial fit width was set to 300, with a minimum with of 200 and a maximum width of 400. The average for an image was calculated to be 246.81±10.67 nm (based on 218581 localizations). This parameter was tested on different frames and optimized using all frames selected. This analysis yielded a molecule list in binary format from which multiple emitters are automatically discarded prior to analysis. STORM NIS-software renders a molecule list in binary format whose coordinates are translated into an image. STORM images are shown in cross or gaussian display mode in Nikon software. Cross takes into account directly the localizations while Gaussian, the one used in our case, is a Gaussian rendering of the localizations considering lateral localization accuracy (with an average of 17.9 ± 4.6) for each localization.

Imaging the gel: During acquisition few signals coming from the free (non-attached) Cy5FF are localized. This noise signal is much weaker than the signal coming from binding events because in this case the probe is immobilized for a long period. For this reason, we set a intensity threshold of the signal to reconstruct the image with the brighter events minimizing the noise.

Also, we obtained better results in apparent lower density areas, especially in the borders of the gel. Imaging the inner parts of the gel by PAINT was not possible even though we were able to image by low resolution TIRF microscopy. We attribute this behaviour to the very low diffusion of the probes inside the gel.

Width measure: in order to emphasise the possibilities we performed the same kind of fiber width measurement made in figure 3c, but using the low res image. First of all, we can only differentiate three fibres, instead of 5. The width measured for fiber 1, 2 and 3 are 488 nm ±46 nm, 505 nm ±37 nm and 411 nm ±50 nm. The results yielded from analysing the low-resolution image show an increase in both size and standard deviation. Also, we want to highlight that like this we observe no difference among fibres width, while using the high-resolution image we could observe those differences.

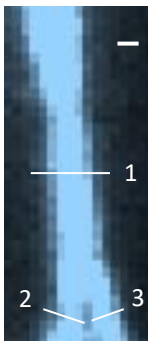

Figure S2. Zoom in of a low-resolution image, corresponding to the same field as in Fig 3 c. Scale bar: 200 nm.

Small Angle Neutron Scattering

To fit the SANS data, the following scattering length densities (SLDs) were used:

FmocFF: 2.757 x 10^{-6} Å^{-2}

D_2O: 6.393 x 10^{-6} Å^{-2}

d_6-DMSO: 5.278 x 10^{-6} Å^{-2}

The SLDs were calculated using the software available from NIST.[3] An assumed density of 1.58 g/mL was used for FmocFF.

The scattering data fit best to a flexible elliptical cylinder model combined with a power law to take into account the scattering at low Q; this combined model was generated in SASView.[1] The data can also be fitted to a flexible cylinder with a power law, but in this case, it is necessary to include a significant polydispersity in the radius (0.3) to access a reasonable fit and, even then, the fit is not as good as to the flexible elliptical cylinder model. As such, the flexible elliptical cylinder and power law model was used. The parameters from this fit are shown in Table S1.

	20:80 DMSO: D_2O	**40:60 DMSO: D_2O**
Background (cm^{-1})	0.00005*	0.00005*

Scale (power law)	$5.18 \times 10^{-6} \pm 5.24 \times 10^{-7}$	$1.80 \times 10^{-6} \pm 4.21 \times 10^{-7}$
Power Law	2.83 ± 0.01	2.90 ± 0.01
Scale (flexible elliptical cylinder)	$6.69 \times 10^{-4} \pm 5.23 \times 10^{-5}$	$4.35 \times 10^{-4} \pm 1.58 \times 10^{-5}$
Length (Å)	1448 ± 16	1458 ± 16
Kuhn Length (Å)	89 ± 1.3	85 ± 1.8
Radius (Å)	33.5 ± 0.1	33.1 ± 0.2
Axis Ratio	2.24 ± 0.01	2.26 ± 0.02
$\chi 2$	3.5674	1.777

Table S1. Fit parameters obtained from a fit to the SANS data using a flexible elliptical cylinder model combined with a power law.* indicates the value was fixed for the fitting procedure.

References

1. www.sasview.org).
2. H. Deschout, F. C. Zanacchi, M. Mlodzianoski, A. Diaspro, J. Bewersdorf, S. T. Hess and K. Braeckmans, *Nature Methods*, 2014, **11**, 253-266.
3. https://www.ncnr.nist.gov/resources/activation/).